*Journal of Breast Imaging*, 2024, Vol. 6, No. 5, 465–475
doi:10.1093/jbi/wbae043
Scientific Review
Received: December 15, 2023; Editorial Decision: May 25, 2024
Published Online: August 31, 2024

Scientific Review

# Dedicated Breast CT: Getting Ready for Prime Time

**Shadi Aminololama-Shakeri, MD, FSBI[1,*] and John M. Boone, PhD, FSBI[1]**

[1]Department of Radiology, University of California, Davis, Sacramento, CA, USA

[*]Corresponding author: Shadi Aminololama-Shakeri (sshakeri@ucdavis.edu)

## Abstract

Dedicated breast CT is an imaging modality that provides true 3D imaging of the breast with many advantages over current conventional breast imaging modalities. The addition of intravascular contrast increases the sensitivity of breast CT substantially. As such, there are immediate potential applications in the clinical workflow. These include using breast CT to replace much of the traditional diagnostic workup when faced with indeterminate breast lesions. Contrast-enhanced breast CT may be appropriate as a supplemental screening tool for women at high risk of breast cancer, similar to breast MRI. In addition, emerging studies are demonstrating the utility of breast CT in neoadjuvant chemotherapy tumor response monitoring as well as planning for surgical treatment options. While short exam times and fully 3D imaging in a noncompressed position are advantages of this modality, limited coverage of chest wall/axilla due to prone positioning and use of ionizing radiation are drawbacks. To date, several studies have reported on the performance characteristics of this promising modality.

**Key words:** CT; breast imaging; breast CT; breast mass; microcalcifications; screening; diagnostic breast imaging; breast cancer; mammography; cone-beam CT; contrast-enhanced breast CT; noncontrast breast CT.

## Introduction

Dedicated breast CT (bCT) provides true 3D imaging of the breast. (The term bCT is used here to describe this technology in general terms; contrast-enhanced bCT [CEbCT] refers specifically to contrast-enhanced studies, and non-CEbCT is specified when needed.)

The advantages of bCT over conventional breast imaging include short exam times, low radiation doses on par with mammography,[1-4] independence of operator skill unlike sonography, noncompressed breast positioning, and minimal susceptibility to the masking effects of breast density. Studies to date have demonstrated superiority to 2D mammography for evaluation of masses[5] as well as increased specificity for detection of malignant microcalcifications when bCT is enhanced with contrast.[6] Enhancement of lesions on intravenous CEbCT reflects tumor vascularity while providing isotropic images and 3D postprocessing capabilities. In addition, preliminary studies have shown the utility of bCT for neoadjuvant treatment monitoring and guiding clinical decisions preoperatively to aid in treatment planning.[7] There is ongoing investigation of bCT radiomics for the prediction of tumor biomarkers and response to therapy. Disadvantages of bCT systems include limited coverage of the chest wall and axilla due to the geometry of prone positioning with the breast in pendant position, limited direct visualization of microcalcifications, and the use of ionizing radiation. While CEbCT has the additional risk of iodinated-contrast injection, most MRI protocols also involve gadolinium-based contrast administration. To date, no large studies have been performed to compare bCT with mammography as a screening modality.

## Protocols and physics

### Breast CT hardware development

The notion of CT imaging of the breast has been considered since the earliest days of CT, dating back to the late 1970s. At the time, General Electric Corporation produced an early

**Key Messages**

- Contrast-enhanced breast CT has improved sensitivity and specificity compared with noncontrast breast CT as well as mammography.
- Breast CT produces isotropic, fully 3D imaging of the breast and has biopsy capability similar to stereotactic biopsy procedures.
- Breast CT has been shown to be a useful imaging modality for neoadjuvant chemotherapy response monitoring.
- Breast CT imaging features may be predictive of molecular tumor subtypes.

prone bCT prototype with the limited technology available at that time. These prototype scanners produced 10-mm section thicknesses, with large voxel dimensions (1.5 mm × 1.5 mm) and large gaps between reconstructed sections. An early clinical study using this technology demonstrated that with contrast enhancement, this very crude bCT system was capable of breast cancer detection similar to that of 2D mammography at that time.[8]

One early bCT system was developed at the University of California, Davis (UC Davis), with 4 generations of prototype scanners, each one improved over the last.[2] Two of these bCT systems also had PET capabilities. The first of these prototypes performed the first cone-beam bCT study on a live patient on November 22, 2004. These 4 scanners all use flat-panel detectors and a cone-beam CT geometry where the breast to be imaged is positioned in pendant geometry through an opening in the tabletop. The first 2 generations of these scanners use a thin-film transistor (TFT) flat-panel detector with a 30-frames-per-second acquisition rate and acquired 500 projection images for total acquisition time of 16.7 seconds. The detector element dimension with 2 × 2 pixel binning was 0.384 mm with these 2 early scanners. The 2 most recently developed prototype scanners use an advanced pulsed x-ray system that improves spatial resolution by dramatically reducing the "motion blur" caused by source rotation. The fourth bCT scanner also has a complementary metal-oxide semiconductor–based flat-panel detector that significantly lowers electronic noise compared with TFT-based flat-panel detectors, smaller detector elements (0.15 mm × 0.15 mm at the detector) leading to better spatial resolution, and much higher frame rate (48 frames per second). All of these parameters improve the image quality performance of cone-beam CT scanners. The fourth prototype bCT system acquires 500 frames in a ~11-second acquisition over 360° gantry rotation and produces bCT images with measurable resolution of 0.150-mm voxel sizes. This bCT technology has been licensed to a company with a commercial scanner in production to be used in U.S. Food and Drug Administration (FDA) trials.

The first commercial bCT scanner (Koning Corporation, West Henrietta, NY) was available for clinical imaging in 2015 after approval by the FDA.[9] The Koning scanner has seen design changes from its original release. This scanner had a similar tabletop as described above for the imaging of the pendant breast. The CT apparatus underneath the tabletop used a flat-panel detector with 360° gantry rotation over a ~10-second acquisition collecting 300 projection images. The projection images were then reconstructed using proprietary CT reconstruction algorithms to produce a high-resolution 3D volume dataset. This scanner used a pulsed x-ray source, which reduces source motion, leading to better spatial resolution. The flat-panel detector on cone-beam bCT systems had an important role in system performance and image quality by decreasing electronic noise and increasing frame rate—both key factors in the improvement of image quality for cone-beam bCT.

A third system was developed and is currently available in Europe for clinical imaging (Advanced Breast CT – ABCT, Nuremberg, Germany). This system does not use cone-beam CT geometry or a flat-panel detector but rather uses high-resolution, solid-state, photon-counting detectors arranged in an arc, similar to the geometry of whole-body CT systems but using horizontal geometry.[10] Patient positioning is identical to the other 2 systems described with the breast placed pendant through an opening in the table. This system has a narrow *z*-axis field of view (~20 mm in the *z* dimension) and uses a helical acquisition geometry, which requires multiple rotations to acquire the full dataset covering the entire length of the breast. The photon-counting detectors add significant cost to the scanner; however, this technology does allow for low-dose acquisition because these photon-counting detectors have very low electronic noise levels. This system has a detector element size of 0.100 mm at the detector. The narrow beam geometry may reduce scattered radiation as well. The detectors also have readout speeds much faster than those of flat-panel detectors, allowing the gantry to rotate much faster (~2-second rotation). However, due to the helical geometry, to cover a 14 cm–long breast, a total of 7 or 8 gantry rotations are required, leading to a 14- to 16-second total acquisition time. The fast detector readout time allows for a nonpulsed (continuous) x-ray beam during scanning.

## Radiation dose to the breast (mean glandular dose)

The calculation of radiation dose to the breast in the bCT prone geometry is completely different than the methods used for mammography or tomosynthesis. For bCT, the x-ray source rotates 360° around the breast, so there is no well-defined "entrance skin air kerma" as with mammography. Instead, the air kerma is measured with a point detector at the center of the field of view (with no phantom present). Monte Carlo methods (computer simulation involving millions of virtual x-ray photons) are used to calculate the mean glandular dose to the breast, and these simulations also take

into consideration the rotational geometry of bCT acquisition. The Monte Carlo studies also determine the air kerma at the center of the field of view, and thus, dose coefficients can be computed to allow the mean glandular dose to be computed from the (measured) air kerma at the center of the field for a complete rotation of the gantry. The many parameters required for accurate breast dosimetry in this geometry include the shape of the x-ray spectrum, the diameter of the breast, the overall scan geometry, and the breast density. The first early attempt at developing coefficients for computing mean glandular dose in the bCT geometry was performed with the assumption that the breast was cylindrical in shape.[11] Fifteen years later, hundreds of volumetric bCT images were used to characterize the actual size and shape of the breast, and Monte Carlo studies were used to update the dose coefficients using this more realistic model of the breast over a range of 5 different realistic breast shapes and sizes.[12]

For many years, it was thought that bCT would be prohibitive in terms of radiation dose. With the special geometry and pendant position of the breast in dedicated bCT scanners, radiation is largely confined to the breast. This means that the x-ray beam need only penetrate the relatively small-diameter breast, not the entire thorax containing the heart, lungs, and ribs of the patient. Breast diameters (measured near the chest wall) in the pendant geometry range from about 10 to 18 cm, with a median breast diameter of 14 cm.[11] Breast tissue is predominantly adipose (average ~84%) even in dense breasts. The lower density of adipose tissue enables higher x-ray beam transmission and thus reduced dose compared with denser tissues, such as muscle or liver. Most significantly, all bCT scanners use much harder x-ray spectra than those used with mammography or tomosynthesis. Radiation dose levels for CEbCT are similar to 2-view 2D mammography for each breast scanned. Radiation dose levels for contrast-enhanced mammography (CEM) have been reported to be 20% to 45% higher than those delivered by 2D mammography.[13,14] Each CEM view (ie, craniocaudal [CC] or mediolateral oblique [MLO]) requires 2 acquisitions because it is a dual-energy procedure requiring both low- and high-kV acquisitions. Thus, MLO and CC contrast-enhanced mammograms of a single breast require 4 acquisitions. The current commercially available bCT scanner (Koning) in the United States uses a 49-kV x-ray spectrum filtered with aluminum, and the other 2 systems described use 60- to 80-kV x-ray spectra. The use of these higher-energy x-ray beams significantly reduces the radiation dose to the breast in dedicated bCT compared with the use of mammography x-ray beams—indeed, if typical mammography spectra (eg, 28 kV) were used in bCT, the radiation doses would be prohibitively high given the large number (300–500) of projection images acquired in bCT. While the higher effective energy of the bCT x-ray beam fundamentally reduces the contrast of microcalcifications compared with mammography, their higher density compared with breast tissue enables microcalcification detectability.

## Spatial resolution in bCT

Digital mammography was developed after years of optimizing screen-film mammography systems for breast imaging. Much of these optimization efforts in the 1990s involved increasing the spatial resolution of mammography. The dedicated mammography systems used small x-ray tube focal spots, and the screen-film cassettes were single-sided and used a very thin layer of scintillator, which limited lateral light spread and improved spatial resolution. The thin scintillator material still allowed adequate x-ray absorption due to the low-energy x-ray spectra (eg, 22-30 kV, Mo/Mo anode filter combination) used in the screen-film era. When digital x-ray mammography systems were initially developed, the low-energy x-ray spectra, small focal spots, and thin scintillator layers were used as with screen-film systems. One mammography system company later developed direct-conversion detector systems made of selenium, and these improved spatial resolution over scintillator-based systems by eliminating lateral light spread.

While the goal of all bCT systems is also to deliver high spatial resolution, the 3D nature of bCT requires compromises not required in projection mammography. CT images are mathematically reconstructed from the 300 to 500 acquired projection images, and these algorithms necessarily perform image preprocessing resulting in "high-pass" filtering of the image data, meaning that smaller structures are amplified in contrast to larger structures. Because x-ray quantum noise is a high-frequency phenomenon, the x-ray quantum noise is amplified during the reconstruction process. Modern artificial intelligence techniques, however, are being deployed to significantly reduce the high-pass noise in all CT images with excellent performance, including in bCT.

The concept of spatial resolution is different in 2D imaging compared with 3D imaging. For example, the 2D mammography system deploying 0.070-mm detector elements can produce excellent spatial resolution in the $x$ and $y$ dimensions (in the 2D mammography planar image); however, at each 2D ($x$, $y$) location on the image, the $z$-axis of the voxel dimension corresponds to the thickness of the compressed breast, ranging from 20 to 90 mm. The volume element in this case, for example, with a typical 50-mm compressed breast thickness, is $0.07 \times 0.07 \times 50$ mm $= 0.245$ mm$^3$. A typical bCT image with 0.150-mm isotropic resolution (in all 3 dimensions) corresponds to a volume element of $(0.150^3) = 0.003375$ mm$^3$. Thus, the bCT volume element is 72 times smaller than that of mammography. The much smaller voxel enables bCT images to largely overcome the issue of overlapping structures, leading to better lesion detection, especially in dense breasts. However, the area of the 2D pixels in ($x$, $y$) in bCT is $0.150^2/0.070^2 = 4.6\times$ larger than mammography. This means that, while 2D mammography is excellent for visualization of very small structures such as microcalcifications, the thin-slice images in 3D bCT significantly reduce the anatomical clutter (also known as the "anatomical noise") associated with dense breasts, leading

to better detection of masses and architectural distortion.[15] While the use of limited-angle tomography, known as breast tomosynthesis, can also reduce anatomical noise, the anatomical noise in tomosynthesis remains similar to that of 2D breast imaging.

## Clinical applications of bCT

Dedicated prone bCT with or without contrast enhancement offers a potential alternative to conventional diagnostic breast imaging.[16] A typical diagnostic workup may include spot compression or magnification views and often US to decide the next steps toward definitive diagnosis and clinical management. The 3D nature of bCT serves to uncover summation and elucidate the characteristics of asymmetries, masses, microcalcifications, and architectural distortion. The isotropic, fully 3D capability of dedicated bCT when coupled with contrast enhancement can provide anatomic as well as vascular information in a manner similar to other contrast-based imaging such as breast MRI and CEM.

In early clinical testing, noncontrast bCT outperformed 2D mammography for visualization of masses.[15] Several ensuing studies have now shown the sensitivity of noncontrast bCT to be better than that of 2D mammography (see Table 1). In a more recent masked retrospective study, 2 experienced mammography readers with 1 year of experience in bCT evaluated 112 Breast Imaging Reporting and Data System (BI-RADS) 4 or 5 masses, 66% (74) of which were malignant.[18] While the sensitivity of bCT (91% reader 1, 88% reader 2) was higher than that of 2D mammography (68% both readers; $P<.001$), the specificity of bCT (34% reader 1, 31% reader 2; $P<.001$) was lower than that of 2D mammography (83% reader 1, 80% reader 2) across breast densities.

### Microcalcifications

Unlike the improvement in the conspicuity of masses with bCT, initial clinical experience showed calcification visualization to be superior on 2D mammography compared with noncontrast bCT.[15] This is not surprising given the higher spatial resolution of mammography. The underperformance of unenhanced bCT in the visualization of microcalcifications in earlier scanners has at least partially been the driving force to improve this technology by increasing the spatial resolution (the fourth UC Davis prototype has about 3 times the spatial resolution as the first 2 prototypes) and further investigate CEbCT.[15,23] While changing techniques, such as increasing the dose or CT slice thickness, improves calcification conspicuity on bCT, the introduction of contrast improves the specificity for malignant calcifications.[1,6,17,25] While malignant microcalcifications due to ductal carcinoma in situ are often seen as enhancing lesions on CEbCT, benign calcifications are not well visualized due to low or lack of enhancement (Figure 1).[6,24]

### Contrast-enhanced bCT

One of the first clinical studies using CEbCT reported that malignant findings were better visualized with CEbCT than unenhanced bCT or mammography.[5] This study of 54 BI-RADS 4 or 5 lesions (25 benign, 29 malignant) also showed that CEbCT differentiated malignant and benign findings based on the degree of enhancement. In that seminal study by Prionas et al,[5] benign findings measured an average of 18 Hounsfield units (HU), which was significantly lower than the average enhancement of malignant lesions, which measured 56 HU. This enhancement differential observed on CEbCT is advantageous for characterizing benign and malignant breast lesions.[21]

Multiple studies have since reported on the diagnostic performance of CEbCT (Table 1). He et al found that CEbCT improved cancer diagnostic sensitivity by 20.3% over noncontrast bCT, mammogram, and US in the diagnostic setting when evaluating 270 lesions in 120 patients with American College of Radiology c or d breast density.[17] Similarly, Wienbeck and colleagues have reported improved sensitivity of CEbCT over bCT and mammography. Additionally, they found that CEbCT accuracy was comparable to MRI (Figure 2) when 2 readers prospectively compared 100 lesions (51 malignant, 6 high risk, and 43 benign) in a masked fashion in women with dense breasts. Contrast-enhanced bCT sensitivity (0.88/0.78 for readers 1 and 2, respectively) was 37% to 39% higher in comparison with mammogram (0.49/0.41, $P<.001$) but not when compared with MRI (0.98/0.96, $P=.0253/.0027$). Specificity of CEbCT (0.71/0.71) was not statistically significantly ($P=.0956$) higher compared with MRI (0.61/0.69, $P=.0956/.7389$).[19]

A recent meta-analysis summarizing the diagnostic accuracy of bCT included 5 noncontrast and 3 contrast-enhanced studies.[26] Contrast-enhanced bCT is reported to have higher pooled sensitivity of 0.899 (95% CI, 0.785-0.956) and pooled specificity of 0.788 (95% CI, 0.709-0.85) compared with noncontrast bCT at 0.789 (95% CI, 0.66–0.89) and 0.697 (95% CI, 0.471-0.851), respectively. These results are limited given the small number of studies available and small sample sizes. In this still-developing field, the bCT literature comprises heterogeneous study design with inclusion of a varying number of subjects. The study participants range in their characteristics including age, breast density, menopausal status, and risk factors, with a mix of lesions including both masses and calcifications.

## Breast density, background parenchymal enhancement, and contrast timing

Adequacy of noncontrast bCT for assessment of parenchymal density has been previously demonstrated.[27] However, unlike mammography, the sensitivity of bCT is not reduced by increasing breast density.[18,28,29] This may be attributed to the 3D nature of bCT allowing for cross-sectional examination of breast tissues in 3 orthogonal thin CT sections. Leafing through

**Table 1.** Characteristics of Unenhanced and CEbCT Performance Studies

| Authors | Number of points | Readers | Masses | Calcifications | bCT/CEbCT | Comparison modality | Design | Malignant lesions | Benign lesions |
|---|---|---|---|---|---|---|---|---|---|
| He et al[17] | 212 | 2 | 260 | 62 | bCT AUC 0.846; CEbCT AUC 0.869 | DM AUC 0.782; US AUC 0.834; $P = .00$ | Prospective | 110 | 332 |
| Aminololama-Shakeri et al[6] | 39 | 2 | - | 39 | CEbCT CS $8.5 \pm 0.9^2$ | DM CS $8.7 \pm 0.8^2$; $P = .85$ | Retrospective | 17 | 22 |
| Wienbeck et al[18] | 59 | 2 | 94 | 18 masses + calcifications | bCT AUC (95% CI): R1, 0.63 (0.54-0.71); R2, 0.60 (0.51-0.68) | DM AUC (95% CI): R1, 0.75 (0.67-0.83); R2: 0.74 (0.65-0.82), $P = .02$ | Retrospective | 74 | 35 (8 bx proven, remainder by follow-up or MRI) |
| Wienbeck et al[19] | 41 (of 100 lesions, 41 were occult on DM) | 2 | 73 (3 asym, 3 other) | 15 ± asym/arch distortion; 6 masses + calcifications | bCT AUC (95% CI): R1, 0.73 (0.65-0.81); R2, 0.66 (0.58-0.75); CEbCT: R1, 0.83 (0.76-0.9); R2, 0.77 (0.68-0.85) | DM AUC (95% CI): R1, 0.69 (0.61-0.77); R2, 0.64 (0.55-0.72); $P < .05$; MRI: R1, 0.88 (0.82-0.93); $P = .22$; R2, 0.89 (0.84-0.95), $P < .05$ | Prospective | 51 | 49 |
| Seifert et al[20] | 129 | 5 | 59 | 5; 6 masses + calcifications | bCT, 67/70 detected; CEbCT ($n = 23$), 23/23 detected | DM, 66/70 detected | Prospective, feasibility | 70 | 50, 5 atypia |
| Uhlig et al[21] | 31 | 2 | - | - | bCT AUC (95% CI): R1, 0.75 (0.64-0.86); R2, 0.67 (0.55-0.78); CEbCT: R1, 0.88 (0.79-0.96); R2: 0.76 (0.65-0.87), $P < .05$ | - | Prospective | 30 | 27 |
| Zhao et al[22] | 65 | 2 | 85 | - | bCT AUC 0.911 | DM AUC 0.827 $P < .01$ | Retrospective | 45 | 40 |
| Wienbeck et al[23] | 83 | 2 | - | 83 | bCT AUC (95% CI): R1, 0.69 (0.58-0.78); R2, 0.68 (0.57-0.77) | DM AUC (95% CI): R1, 0.78 (0.69-0.85); R2, 0.73 (0.63-0.82), $P = .085$ | Retrospective | 32 | 28 |
| Aminololama-Shakeri et al[24] | 100 | 2 | 51 | 49 | CEbCT CS $9.7 \pm 0.5$,[a] $8.7 \pm 0.8$[b] | DM CS $6.7 \pm 3.0$,[a] $8.8 \pm 0.7$[b]; DBT $6.8 \pm 3.1$,[a] $P < .05$[a]; $8.5 \pm 0.6$,[b] $P =$ NS | Retrospective | 50 | 50 |

Abbreviations: asym, asymmetry; AUC, area under the curve; bCT, breast CT; bx, biopsy digital mammography; CEbCT, contrast-enhanced breast CT; CS, conspicuity score; DBT, digital breast tomosynthesis; DM, digital mammography; NS, not significant.

[a]Results reflect malignant masses.

[b]Results reflect malignant calcifications.

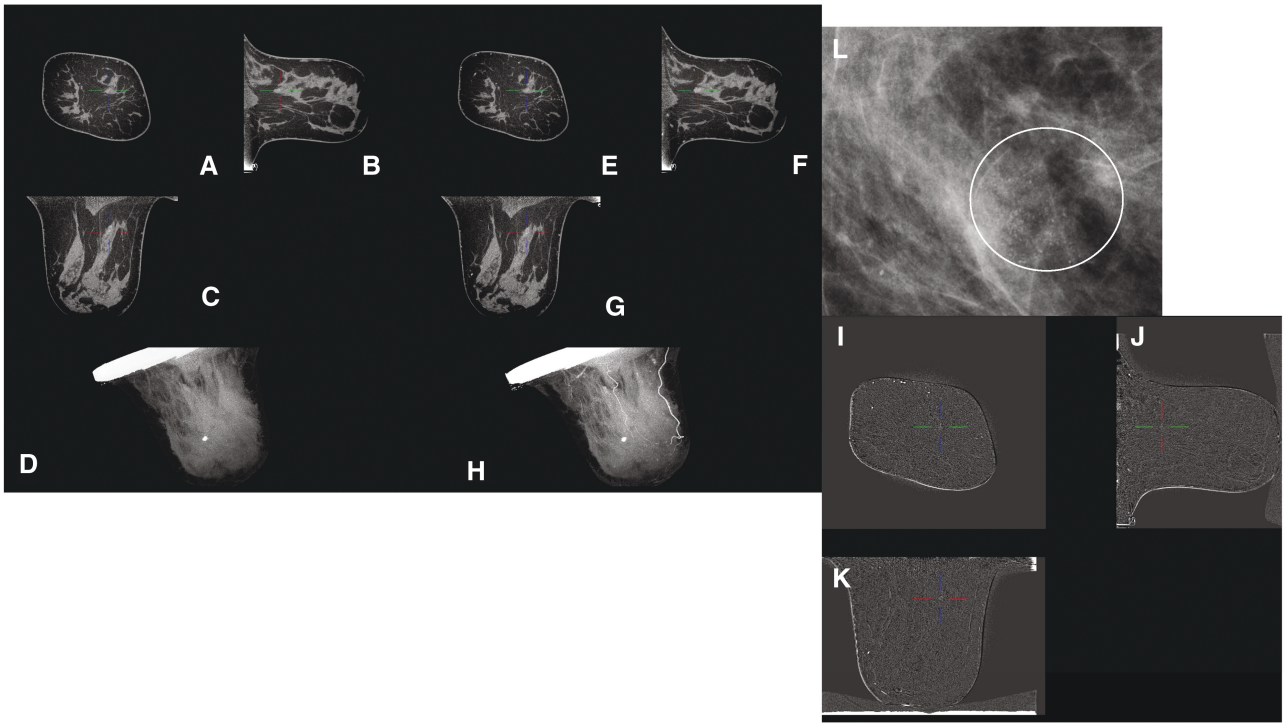


**Figure 1.** Coronal (**A**), sagittal (**B**), axial (**C**), and maximum-intensity projection (MIP) (**D**) noncontrast breast CT (bCT); coronal (**E**), sagittal (**F**), axial (**G**), and MIP (**H**) contrast-enhanced bCT (CEbCT); and subtracted coronal (**I**), sagittal (**J**), and axial (**K**) images demonstrate no discernable lesion to correspond with the group of amorphous microcalcifications (circled) on optical magnified mammogram (**L**), which were columnar cell hyperplasia on core biopsy.

the breast volume in slices with digital breast tomosynthesis allows for separation of tissue overlap and thereby decreased recalls for summation when compared with mammography in large clinical studies.[30-32] Digital breast tomosynthesis, however, produces images based on a limited angle arc of 15° to 60° compared with the true 3D and isotropic bCT images produced by a 360° rotation around the breast.

While there is mounting evidence regarding the importance of the role of background parenchymal enhancement (BPE) in breast MRI, data are sparse regarding BPE in CEbCT.[33] In a retrospective analysis of 221 women, the majority of readers found BPE levels to be lower on CEbCT compared with MRI ($P$ <.001).[34] The analysis in this study was performed based on images obtained at 120 seconds and at 90 seconds after intravenous injection of contrast for bCT and MRI, respectively. A small prospective study of 90 patients with BI-RADS 4 or 5 lesions imaged with CEbCT at an early (70–95 seconds, $n$ = 73) or late (165–492 seconds, $n$ = 17) timepoint after intravenous injection of 100 ml of iodixanol 320 did not find a correlation between the conspicuity of lesions and contrast timing.[35] Fifty of the 90 subjects had qualitative designation of their BPE as minimal, mild, moderate, or marked. Background parenchymal enhancement was not affected by the contrast timing (Figure 3). For optimal differentiation of benign and malignant lesions, Uhlig et al have suggested CEbCT images be obtained 2 minutes after injection of contrast material.[21]

## Breast CT–guided interventions

Initial experience with core biopsy using dedicated bCT guidance was first reported by Seifert and colleagues using anthropomorphic breast biopsy phantoms containing masses and calcifications.[20] Using a similar add-on biopsy platform, feasibility in human subjects has now been demonstrated much akin to stereotactic technique in prone position.[36] Wienbeck et al performed vacuum-assisted biopsies (VABs) in 65 women with 68 nonpalpable BI-RADS category 4 (63/68) or 5 (5/68) lesions. Of those, 31 lesions were biopsied with bCT guidance after an initial scan with the affected breast stabilized in a grid system to identify the target. A second scan was used to confirm the placement of a marker tube, and a third scan was performed postbiopsy and after placement of a biopsy clip, similar to typical MRI-guided biopsy protocols.[36] The remaining 37 lesions were biopsied with prone stereotactic technique. Most of the lesions biopsied were microcalcifications with or without masses; 4/31 (13%) lesions were biopsied under bCT guidance, and 1/37 (3%) using stereotactic technique were noncalcified masses. Two cases of microcalcifications that were not targetable with bCT, 1 due to nonvisualization and the other due to diffuse distribution, were sampled with stereotactic technique. Both were benign. One benign lesion was surgically sampled due to inability to be visualized using stereotactic biopsy and was excluded from the study. No significant time difference

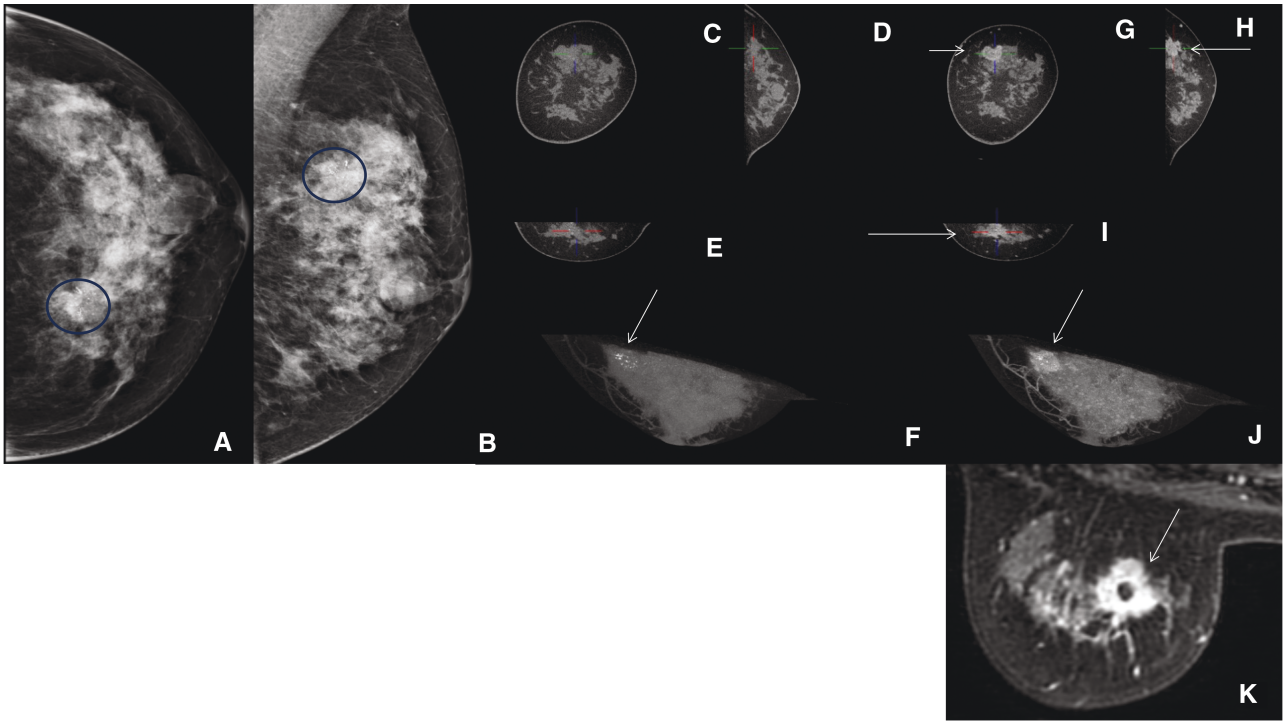


**Figure 2.** Medial mass and calcifications (dark circle) noted on craniocaudal (**A**) and mediolateral oblique (**B**) views. Breast CT (bCT) coronal (**C**), sagittal (**D**), axial (**E**), and maximum-intensity projection (MIP) (**F**) demonstrate calcifications, and contrast-enhanced bCT coronal (**G**), sagittal (**H**), axial (**I**), and MIP (**J**) show calcifications and enhancing irregular mass that was intermediate-grade invasive ductal carcinoma. Axial MRI shows the enhancing malignancy with biopsy clip artifact (**K**).

was found between the 2 biopsy techniques with mean intervention time of 22.7 ± 8.4 minutes for CT and 28 ± 9.4 minutes for stereotactic VAB. There was no significant difference in the mean glandular radiation dose to patients for both biopsy methods (CT 31.7 ± 16.0 mGy, stereotactic 37.7 ± 24.2 mGy). This study demonstrates feasibility of safely using bCT-guided biopsy system with similar dose and intervention time as stereotactic VAB. The authors note significant experience within their practice group utilizing the described CT-guided system for sampling all lesions requiring imaging-guided biopsy not visible at US.

## Neoadjuvant treatment planning and monitoring

Neoadjuvant chemotherapy (NAC) is now the cornerstone of treatment for locally advanced breast cancer in advance of surgery.[37] Tumor response to NAC has been associated with long-term prognosis with pathologic complete response (pCR) being predictive of longer disease-free survival.[38,39] It is therefore highly desirable to identify tumor response accurately and as early as possible to avoid potentially toxic chemotherapy side effects for patients who are nonresponders.[40] Breast CT has been shown to have potential as an imaging modality to help quantify tumor response and direct treatment options. Feasibility of monitoring NAC treatment with noncontrast dedicated bCT was tested in a prospective pilot study by Vedantham et al.[41] Eleven women undergoing NAC were imaged before, at midpoint of, and after receiving 4 cycles of doxorubicin/cyclophosphamide and before 4 cycles of either paclitaxel or the combination of 12 weekly cycles of paclitaxel/trastuzumab for patients with HER2/neu-positive tumors as well as following completion of treatment. Tumor volumes from a single radiologist's tumor boundary markings in several coronal projections were computed and compared with estimations generated from automated segmentation (MATLAB version 8.1, The MathWorks Inc., Natick, MA). Tumors smaller than 5 mm were excluded due to the possibility of presence of beam-hardening artifact from the biopsy clip. Vedantham et al reported a reduction of at least 30% in tumor volume at midtreatment and observed further decrease at final posttreatment scans. While comparatively smaller tumor volumes were observed on bCT than MRI, Vendatham et al reported agreement in temporal volume changes between the 2 modalities. The pCR rate in their study was 27.3% (3/11), in congruence with other reports.[42] This study highlights the potential utility of bCT in a tailored treatment approach without contrast administration for identifying known tumors with potential to predict response to NAC.

In a more recent study of 81 patients undergoing NAC for locally advanced breast cancer using both noncontrast and contrast-enhanced bCT, Chen et al also found that noncontrast bCT–measured parameters such as tumor volume

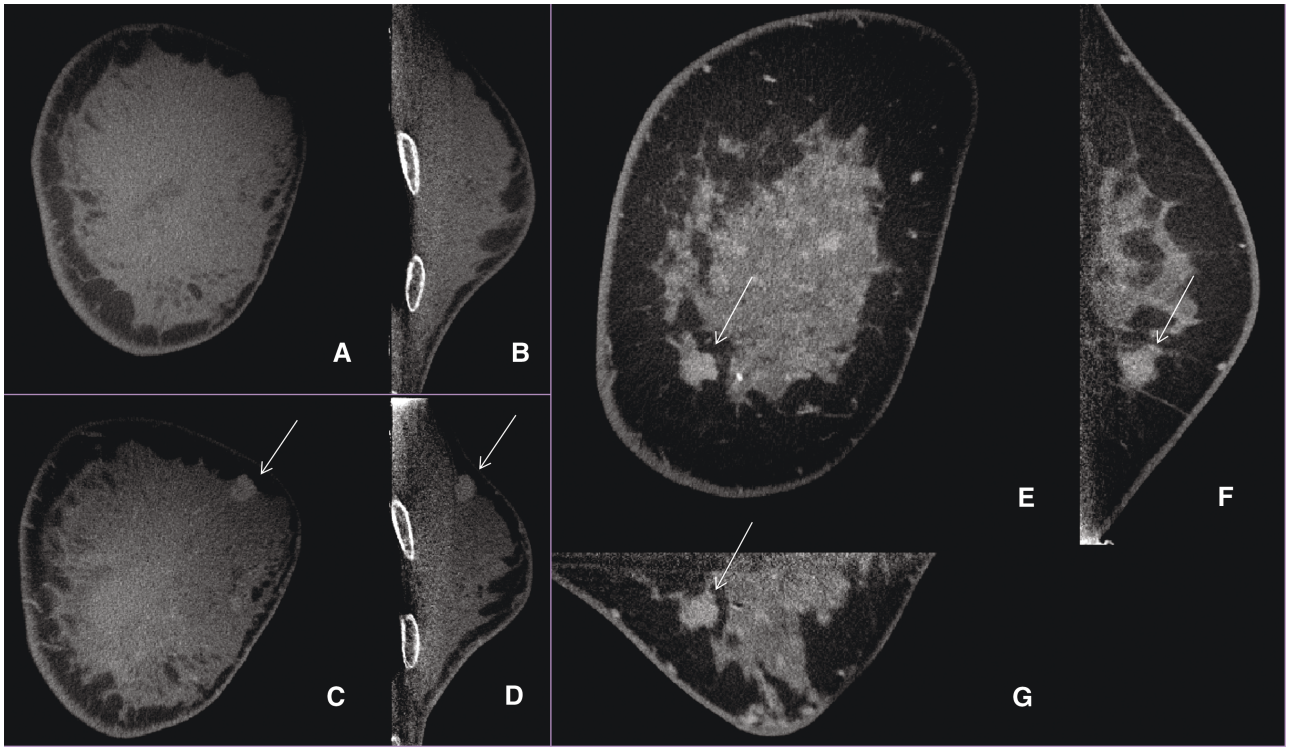


**Figure 3.** Precontrast coronal (**A**) and sagittal (**B**) bCT and postcontrast coronal (**C**) and sagittal (**D**) bCT images in a 55-year-old patient show extremely dense breast tissue. After late contrast delay timing (398 s), a small irregular enhancing mass is seen, which was an invasive ductal carcinoma (white arrows). Note the mild background parenchymal enhancement. Coronal (**E**), sagittal (**F**), and axial (**G**) contrast-enhanced bCT images obtained early (91 s) after contrast injection in a 46-year-old patient show an enhancing mass, which is biopsy-proven intermediate grade invasive ductal carcinoma (white arrows). Note the moderate background parenchymal enhancement.

have potential for predicting tumor response to therapy.[43] The average age of patients in this study was 43.4 years (range of 26 to 67 years) with mean tumor size of 41.3 mm (ranging from 10 to 97 mm), and all patients had a dedicated bCT before NAC initiation. The bCT was repeated after the third cycle (midpoint) of NAC in 55 patients and following 7 cycles (late) in 65 patients. Pathologic complete response was demonstrated in 36 patients (44%). At the midpoint of treatment, the parameters that showed significant difference between the responders and the nonresponder groups included tumor diameter, maximum enhancement ratio, 2-minute enhancement, and hormone status. They report a predictive model based on these features reaching an area under the curve (AUC) of 0.874 for predicting pCR in the group of patients undergoing CT after 7 cycles of treatment.[43] Consistent with other studies,[40] the authors report an accuracy of 81.5% and a sensitivity of 99.6% in predicting the response to NAC. They also suggest that dynamic tumor enhancement could provide additional information in the prediction of tumor response, although reports in MRI have been mixed.[44,45] Most recent data from a study in 91 patients undergoing NAC who were imaged preoperatively with CEbCT and MRI show higher sensitivity with CEbCT but lower specificity than MRI for predicting pCR. Contrast-enhanced bCT was more accurate than MRI, however, when assessing residual tumor particularly with presence of calcifications.[46]

## Tumor subtypes

Breast cancer molecular subtypes may potentially be predicted from imaging features derived from CEbCT.[47-49] In a retrospective analysis of imaging features by 2 radiologists in 211 patients with 240 malignant lesions and mean age of 48.6 ± 10.7 years who underwent preoperative CEbCT, Ma et al report that 11 CEbCT features were associated with immunohistochemistry receptor status, and some of them in combination may be predictive of molecular subtypes. These include lesion type, size, density, degree of enhancement, mass shape, spiculations, internal enhancement pattern, presence and distribution of calcifications, and peripheral vascularity of lesions as well as focality number of lesions.[50] The authors of this study suggest that the combined features could differentiate luminal, HER2-enriched, and triple-negative molecular subtypes of breast cancer. Their study corroborated previously demonstrated results[51] that irregular masses with spiculated margins were associated with hormone receptor–positivity and low Ki-67 proliferation, characteristics with better prognosis. The presence of microcalcifications and increased peripheral vascularity were associated with HER2-enriched breast cancers. In another study, Zhu and colleagues also demonstrated that calcifications, nonmass enhancement (NME), masses associated with NME, and calcifications, particularly extending beyond the lesions, were significantly correlated with HER2/neu overexpression

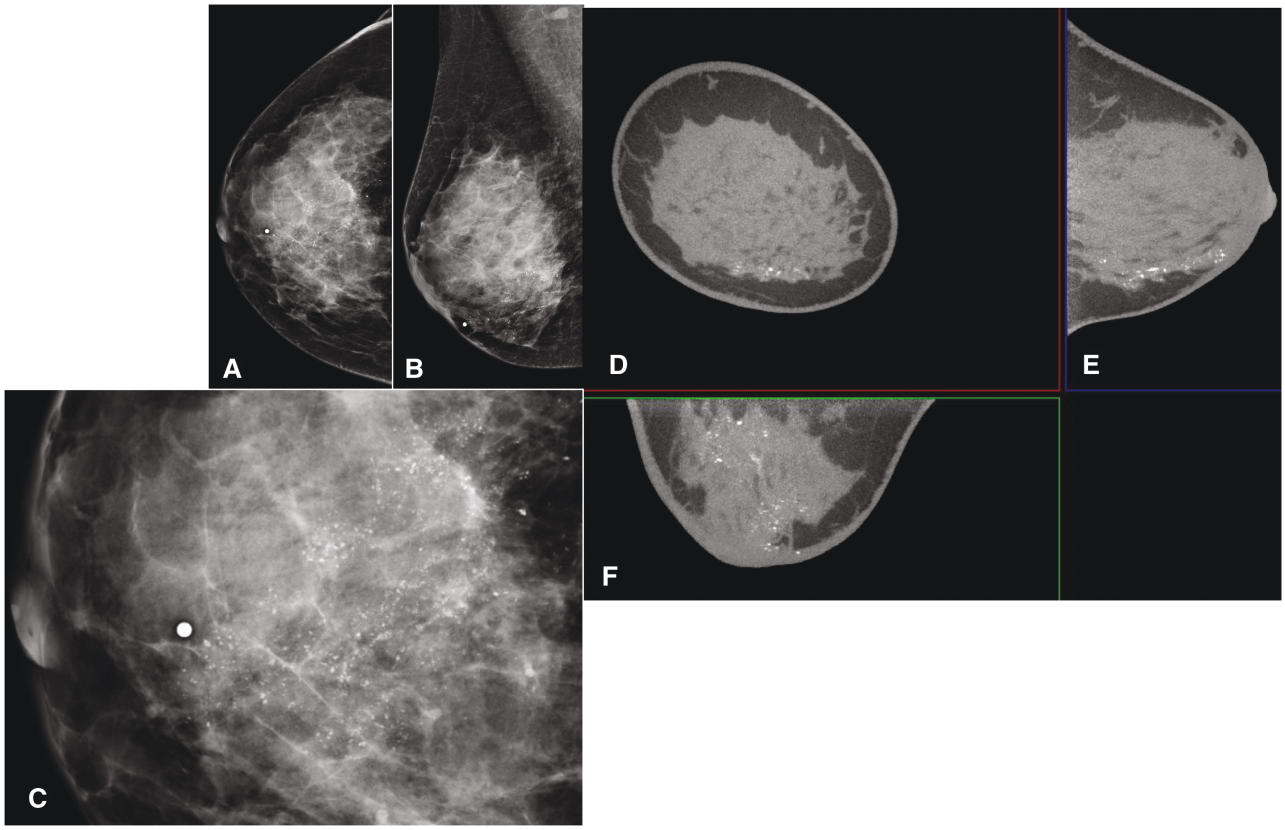


**Figure 4.** Sixty-five-year-old with dense breast tissue and segmentally distributed pleomorphic microcalcifications on craniocaudal (**A**) and mediolateral oblique (**B**) mammogram. **C**: Optical magnified view. Noncontrast breast CT in coronal (**D**), sagittal (**E**), and axial (**F**) images demonstrates the extent of the ductal carcinoma in situ, which was ER+ and PR+ and had Her2/neu overexpression.

($P$ <.05).[52] Interestingly, the distribution of calcifications on bCT may also be associated with molecular subtypes (Figure 4).[50]

## Surgical treatment planning

Contrast-enhanced modalities, such as MRI and, more recently, CEM, are used clinically for determining the extent of malignancy in the preoperative setting. Breast CT may have utility in supporting decision-making regarding breast-conserving therapy vs the need for mastectomy. In a retrospective analysis of 200 women with breast cancer who had undergone imaging with noncontrast bCT, 2 imaging radiologists without knowledge regarding the clinicopathologic or other imaging findings marked the tumor, tissue, and breast for an automated calculation. This report showed an advantage of lower radiation-dose and radiation to the breast only and not to the rest of the body in comparison with prior studies with conventional contrast-enhanced chest CT in the supine position for preoperative planning of the best surgical approach.[53]

## Conclusion and future directions

Breast CT shows promise in diagnostic performance compared with mammography. With contrast enhancement, CEbCT has the potential to improve current diagnostic exam workflows replacing multiple imaging modalities that we use today. Early studies suggest that it is superior for detection of malignant masses and at least equal in visualization of malignant calcifications as mammography. Moreover, potential for increased specificity means that benign lesions may be better recognized as such, thereby potentially improving positive predictive values for biopsy and reducing short-term surveillance. As in other contrast-enhanced modalities, CEbCT may also be utilized to determine extent of malignancy and evaluate response to NAC. Finally, CEbCT is faster to perform and does not require breast compression, improving throughput and patient comfort. Newer generations of bCT are showing improvements in overcoming the limitations of bCT for direct microcalcification visualization and chest wall/axillary tissue coverage. Nevertheless, the studies of bCT to date have been small and have had varying designs. Prospective, blinded, large, multicentered studies are needed to examine whether the demonstrated early benefits of bCT will bear out in larger clinical trials and are ultimately worth the financial investment.

## Funding

None declared.

## Conflict of interest statement

The work performed at UC Davis was all completed on the prototype CT machines. The licensing has now been transferred to

Izotropic. Dr. Shakeri is a consultant for Izotropic. None of the work reported within the submitted manuscript is related to Izotropic. Dr. Boone does not have any conflicts to declare.

## Author contributions

John M. Boone (Conceptualization, Data curation, Formal analysis, Funding acquisition, Investigation, Methodology, Project administration, Resources, Software, Supervision, Validation, Visualization, Writing – original draft, Writing – review & editing, and Shadi Aminololama-Shakeri (Research, Writing – original draft, Writing – review & editing)

## References


1. O'Connell A, Conover DL, Zhang Y, et al. Cone-beam CT for breast imaging: radiation dose, breast coverage, and image quality. *AJR Am J Roentgenol*. 2010;195(2):496-509. doi:10.2214/ajr.08.1017
2. Boone JM, Nelson TR, Lindfors KK, Seibert JA. Dedicated breast CT: radiation dose and image quality evaluation. *Radiology*. 2001;221(3):657-667. doi:10.1148/radiol.2213010334
3. O'Connell AM, Kawakyu-O'Connor D. Dedicated cone-beam breast computed tomography and diagnostic mammography: comparison of radiation dose, patient comfort, and qualitative review of imaging findings in BI-RADS 4 and 5 lesions. *J Clin Imaging Sci*. 2012;2:7. doi:10.4103/2156-7514.93274
4. Boone JM, Kwan AL, Seibert JA, Shah N, Lindfors KK, Nelson TR. Technique factors and their relationship to radiation dose in pendant geometry breast CT. *Med Phys*. 2005;32(12):3767-3776. doi:10.1118/1.2128126
5. Prionas ND, Lindfors KK, Ray S, et al. Contrast-enhanced dedicated breast CT: initial clinical experience. *Radiology*. 2010;256(3):714-723. doi:10.1148/radiol.10092311
6. Aminololama-Shakeri S, Abbey CK, Gazi P, et al. Differentiation of ductal carcinoma in-situ from benign micro-calcifications by dedicated breast computed tomography. *Eur J Radiol*. 2016;85(1):297-303. doi:10.1016/j.ejrad.2015.09.020
7. Li J, Zhong G, Wang K, Kang W, Wei W. Tumor-to-gland volume ratio versus tumor-to-breast ratio as measured on CBBCT: possible predictors of breast-conserving surgery. *Cancer Manag Res*. 2021;13:4463-4471. doi:10.2147/cmar.S312288
8. Gisvold JJ, Karsell PR, Reese EC. Clinical evaluation of computerized tomographic mammography. *Mayo Clin Proc*. 1977;52(3):181-185.
9. Chen B, Ning R. Cone-beam volume CT breast imaging: feasibility study. *Med Phys*. 2002;29(5):755-770. doi:10.1118/1.1461843
10. Kalender WA, Beister M, Boone JM, Kolditz D, Vollmar SV, Weigel MC. High-resolution spiral CT of the breast at very low dose: concept and feasibility considerations. *Eur Radiol*. 2012;22(1):1-8. doi:10.1007/s00330-011-2169-4
11. Boone JM, Shah N, Nelson TR. A comprehensive analysis of $DgN_{CT}$ coefficients for pendant-geometry cone-beam breast computed tomography. *Med Phys*. 2004;31(2):226-235. doi:10.1118/1.1636571
12. Hernandez AM, Becker AE, Boone JM. Updated breast CT dose coefficients ($DgN_{CT}$) using patient-derived breast shapes and heterogeneous fibroglandular distributions. *Med Phys*. 2019;46(3):1455-1466. doi:10.1002/mp.13391
13. Hendrick RE. Radiation doses and risks in breast screening. *J Breast Imaging*. 2020;2(3):188-200. doi:10.1093/jbi/wbaa016
14. Gennaro G, Cozzi A, Schiaffino S, Sardanelli F, Caumo F. Radiation dose of contrast-enhanced mammography: a two-center prospective comparison. *Cancers (Basel)*. 2022;14(7):1774. doi:10.3390/cancers14071774
15. Lindfors KK, Boone JM, Nelson TR, Yang K, Kwan AL, Miller DF. Dedicated breast CT: initial clinical experience. *Radiology*. 2008;246(3):725-733. doi:10.1148/radiol.2463070410
16. O'Connell AM, Karellas A, Vedantham S. The potential role of dedicated 3D breast CT as a diagnostic tool: review and early clinical examples. *Breast J*. 2014;20(6):592-605. doi:10.1111/tbj.12327
17. He N, Wu YP, Kong Y, et al. The utility of breast cone-beam computed tomography, ultrasound, and digital mammography for detecting malignant breast tumors: a prospective study with 212 patients. *Eur J Radiol*. 2016;85(2):392-403. doi:10.1016/j.ejrad.2015.11.029
18. Wienbeck S, Uhlig J, Luftner-Nagel S, et al. The role of cone-beam breast-CT for breast cancer detection relative to breast density. *Eur Radiol*. 2017;27(12):5185-5195. doi:10.1007/s00330-017-4911-z
19. Wienbeck S, Fischer U, Luftner-Nagel S, Lotz J, Uhlig J. Contrast-enhanced cone-beam breast-CT (CBBCT): clinical performance compared to mammography and MRI. *Eur Radiol*. 2018;28(9):3731-3741. doi:10.1007/s00330-018-5376-4
20. Seifert PJ, Morgan RC, Conover DL, Arieno AL. Initial experience with a cone-beam breast computed tomography-guided biopsy system. *J Clin Imaging Sci*. 2017;7:1. doi:10.4103/2156-7514.199055
21. Uhlig J, Fischer U, Surov A, Lotz J, Wienbeck S. Contrast-enhanced cone-beam breast-CT: Analysis of optimal acquisition time for discrimination of breast lesion malignancy. *Eur J Radiol*. 2018;99:9-16. doi:10.1016/j.ejrad.2017.12.003
22. Zhao B, Zhang X, Cai W, Conover D, Ning R. Cone beam breast CT with multiplanar and three dimensional visualization in differentiating breast masses compared with mammography. *Eur J Radiol*. 2015;84(1):48-53. doi:10.1016/j.ejrad.2014.05.032
23. Wienbeck S, Andrijevska V, Kuck F, et al. Comparison between cone-beam breast-CT and full-field digital mammography for microcalcification detection depending on breast density. *Medicine (Baltimore)*. 2023;102(22):e33900. doi:10.1097/MD.0000000000033900
24. Aminololama-Shakeri S, Abbey CK, Lopez JE, et al. Conspicuity of suspicious breast lesions on contrast enhanced breast CT compared to digital breast tomosynthesis and mammography. *Br J Radiol*. 2019;92(1097):20181034. doi:10.1259/bjr.20181034
25. Lai CJ, Shaw CC, Chen L, et al. Visibility of microcalcification in cone beam breast CT: effects of X-ray tube voltage and radiation dose. *Med Phys*. 2007;34(7):2995-3004. doi:10.1118/1.2745921
26. Uhlig J, Uhlig A, Biggemann L, Fischer U, Lotz J, Wienbeck S. Diagnostic accuracy of cone-beam breast computed tomography: a systematic review and diagnostic meta-analysis. *Eur Radiol*. 2019;29(3):1194-1202. doi:10.1007/s00330-018-5711-9
27. Ma Y, Cao Y, Liu A, et al. A reliability comparison of cone-beam breast computed tomography and mammography: breast density assessment referring to the fifth edition of the BI-RADS Atlas. *Acad Radiol*. 2019;26(6):752-759. doi:10.1016/j.acra.2018.07.023

28. Mandelson MT, Oestreicher N, Porter PL, et al. Breast density as a predictor of mammographic detection: comparison of interval- and screen-detected cancers. *J Natl Cancer Inst*. 2000;92(13):1081-1087. doi:10.1093/jnci/92.13.1081
29. Lindfors KK, Boone JM, Newell MS, D'Orsi CJ. Dedicated breast computed tomography: the optimal cross-sectional imaging solution? *Radiol Clin North Am*. 2010;48(5):1043-1054. doi:10.1016/j.rcl.2010.06.001
30. Friedewald SM, Rafferty EA, Rose SL, et al. Breast cancer screening using tomosynthesis in combination with digital mammography. *JAMA*. 2014;311(24):2499-2507. doi:10.1001/jama.2014.6095
31. Ciatto S, Houssami N, Bernardi D, et al. Integration of 3D digital mammography with tomosynthesis for population breast-cancer screening (STORM): a prospective comparison study. *Lancet Oncol*. 2013;14(7):583-589. doi:10.1016/S1470-2045(13)70134-7
32. Skaane P, Bandos AI, Gullien R, et al. Comparison of digital mammography alone and digital mammography plus tomosynthesis in a population-based screening program. *Radiology*. 2013;267(1):47-56. doi:10.1148/radiol.12121373
33. Liao GJ, Henze Bancroft LC, Strigel RM, et al. Background parenchymal enhancement on breast MRI: a comprehensive review. *J Magn Reson Imaging*. 2020;51(1):43-61. doi:10.1002/jmri.26762
34. Ma Y, Liu A, Zhang Y, et al. Comparison of background parenchymal enhancement (BPE) on contrast-enhanced cone-beam breast CT (CE-CBBCT) and breast MRI. *Eur Radiol*. 2022;32(8):5773-5782. doi:10.1007/s00330-022-08699-2
35. Aminololama-Shakeri S, Gazi P, Lindfors K, Boone J. Is lesion depiction on contrast enhanced dedicated breast computed tomography affected by contrast timing? Radiological Society of North America 2013 Scientific Assembly and Annual Meeting. Radiological Society of North America, December 2013;1-6. Accessed August 20, 2023. https://archive.rsna.org/2013/13028366.html
36. Wienbeck S, Lotz J, Fischer U. Feasibility of vacuum-assisted breast cone-beam CT–guided biopsy and comparison with prone stereotactic biopsy. *AJR Am J Roentgenol*. 2017;208(5):1154-1162. doi:10.2214/ajr.16.16760
37. Loibl S, Poortmans P, Morrow M, Denkert C, Curigliano G. Breast cancer. *Lancet*. 2021;397(10286):1750-1769. doi:10.1016/S0140-6736(20)32381-3
38. Chou HH, Chung WS, Ding RY, et al. Factors affecting locoregional recurrence in breast cancer patients undergoing surgery following neoadjuvant treatment. *BMC Surg*. 2021;21(1):160. doi:10.1186/s12893-021-01158-7
39. von Minckwitz G, Untch M, Blohmer JU, et al. Definition and impact of pathologic complete response on prognosis after neoadjuvant chemotherapy in various intrinsic breast cancer subtypes. *J Clin Oncol*. 2012;30(15):1796-1804. doi:10.1200/JCO.2011.38.8595
40. Drisis S, Metens T, Ignatiadis M, Stathopoulos K, Chao SL, Lemort M. Quantitative DCE-MRI for prediction of pathological complete response following neoadjuvant treatment for locally advanced breast cancer: the impact of breast cancer subtypes on the diagnostic accuracy. *Eur Radiol*. 2016;26(5):1474-1484. doi:10.1007/s00330-015-3948-0
41. Vedantham S, O'Connell AM, Shi L, Karellas A, Huston AJ, Skinner KA. Dedicated breast CT: feasibility for monitoring neoadjuvant chemotherapy treatment. *J Clin Imaging Sci*. 2014;4:64.
42. Rastogi P, Anderson SJ, Bear HD, et al. Preoperative chemotherapy: updates of National Surgical Adjuvant Breast and Bowel Project Protocols B-18 and B-27. *J Clin Oncol*. 2008;26(5):778-785. doi:10.1200/JCO.2007.15.0235
43. Chen S, Li S, Zhou C, et al. Assessment of cone-beam breast computed tomography for predicting pathologic response to neoadjuvant chemotherapy in breast cancer: a prospective study. *J Oncol*. 2022;2022:9321763. doi:10.1155/2022/9321763
44. Ohashi A, Kataoka M, Iima M, et al. A multiparametric approach to diagnosing breast lesions using diffusion-weighted imaging and ultrafast dynamic contrast-enhanced MRI. *Magn Reson Imaging*. 2020;71:154-160. doi:10.1016/j.mri.2020.04.008
45. Wu J, Gong G, Cui Y, Li R. Intratumor partitioning and texture analysis of dynamic contrast-enhanced (DCE)-MRI identifies relevant tumor subregions to predict pathological response of breast cancer to neoadjuvant chemotherapy. *J Magn Reson Imaging*. 2016;44(5):1107-1115. doi:10.1002/jmri.25279
46. Wang Y, Zhao M, Ma Y, et al. Accuracy of preoperative contrast-enhanced cone beam breast CT in assessment of residual tumor after neoadjuvant chemotherapy: a comparative study with breast MRI. *Acad Radiol*. 2023;30(9):1805-1815. doi:10.1016/j.acra.2022.12.027
47. Ma WM, Li J, Chen SG, et al. Correlation between contrast-enhanced cone-beam breast computed tomography features and prognostic staging in breast cancer. *Br J Radiol*. 2022;95(1132):20210466. doi:10.1259/bjr.20210466
48. Uhlig J, Fischer U, von Fintel E, et al. Contrast enhancement on cone-beam breast-CT for discrimination of breast cancer immunohistochemical subtypes. *Transl Oncol*. 2017;10(6):904-910. doi:10.1016/j.tranon.2017.08.010
49. Chen JT, Zhou CY, He N, Wu YP. Optimal acquisition time to discriminate between breast cancer subtypes with contrast-enhanced cone-beam CT. *Diagn Interv Imaging*. 2020;101(6):391-399. doi:10.1016/j.diii.2020.01.001
50. Ma Y, Liu A, O'Connell AM, et al. Contrast-enhanced cone beam breast CT features of breast cancers: correlation with immunohistochemical receptors and molecular subtypes. *Eur Radiol*. 2021;31(4):2580-2589. doi:10.1007/s00330-020-07277-8
51. Bae MS, Seo M, Kim KG, Park IA, Moon WK. Quantitative MRI morphology of invasive breast cancer: correlation with immunohistochemical biomarkers and subtypes. *Acta Radiol*. 2015;56(3):269-275. doi:10.1177/0284185114524197
52. Zhu Y, Zhang Y, Ma Y, et al. Cone-beam breast CT features associated with HER2/neu overexpression in patients with primary breast cancer. *Eur Radiol*. 2020;30(5):2731-2739. doi:10.1007/s00330-019-06587-w
53. Akashi-Tanaka S, Sato N, Ohsumi S, et al. Evaluation of the usefulness of breast CT imaging in delineating tumor extent and guiding surgical management: a prospective multi-institutional study. *Ann Surg*. 2012;256(1):157-162. doi:10.1097/SLA.0b013e31825b6cb1